JOURNAL OF Applied Polymer SCIENCE

Simulation and Application of Response Surface Methodology to a Nylon-6 Hydrolytic Polymerization in a Semibatch Reactor

Vanessa Ito Funai, Delba Nisi Cosme Melo, Nádson Murilo Nascimento Lima, Rubens Maciel Filho
Department of Chemical Process, LOPCA/UNICAMP, Laboratory of Optimization, Design and Advanced Control, School of Chemical Engineering, University of Campinas, UNICAMP, Campinas-SP 13083-852, Brazil

Correspondence to: V. I. Funai (E-mail: vanfunai@yahoo.com.br)

ABSTRACT: This work presents an experimental design methodology combined with computational simulation to correlate the influence of operational conditions and reactants charge in the numeric average molecular weight (MWN) as well as on monomer conversion (X_{CL}), for the hydrolytic polymerization of nylon-6 in a semibatch reactor. It evaluated the reaction temperature, the pressure profile, and the proportion of reactants in the charge. Experimental design was used to screen the most statistically significant variables and to develop a reliable predictive model for each response. The combined use of the models can be applied for process optimization, by establishing MWN and maximum X_{CL} as objective functions. Responses surface allowed the visualization of the responses behavior when changing the independent variables and therefore to identify the optimal tendencies. This work demonstrates that such methodology can be applied for optimization of complex processes like the hydrolytic polymerization of nylon-6. This polymerization has many side reactions occurring at the same time, which are sensitive to different profiles of pressure and temperature that are applied. This evaluation is quite interesting as such profiles are necessary to perform the several polymerization steps and have a significant impact on product characteristics and therefore in its applications. © 2012 Wiley Periodicals, Inc. J. Appl. Polym. Sci. 000: 000–000, 2012

KEYWORDS: nylon; simulations; step-growth polymerization; experimental design

Received 23 July 2011; accepted 14 March 2012; published online
DOI: 10.1002/app.37697

INTRODUCTION

Nylon is considered the first polymer in the category of engineering plastics and still remains as one of the most important since its discovery, in 1935. It is widely used as raw material in the fibers and engineering plastics manufacturing and its application includes many different sectors, like textiles, automobiles, electrical appliances, among others.[1] Nylon 6 is the most manufactured polyamide, however most of its production ends in the fibers market, which is already saturated; thus, it is necessary to find new applications for polyamides as engineering plastics. As far as process is concerned, there are two main routes for nylon-6 polymerization, namely anionic and hydrolytic. The hydrolytic route is the more used for commercial production.[1]

To have a final product with desired properties, it is necessary to have a better comprehension of the polymerization process, including the reactor performance, and this can be performed through mathematical modeling and computer simulation. Wajge et al.[2] studied the simulation of a semibatch reactor using water and ε-caprolactam and predicted several molecular characteristics of the polymer; however, they were related to characterizing parameters of the reactor, like mass and heat transfer, reaction kinetics, and jacket fluid temperature. Tang et al.[3] simulated the hydrolytic polymerization of ε-caprolactam using bifunctional regulators and analyzed characteristic data of the polymerization like conversion, polydispersity index (PDI), average molecular weight, and species concentration; it was found that the presence of more bifunctional acid decreases the PDI while, in the case of monofunctional acid, the PDI asymptotically reaches a value of 2 regardless of the amount of monofunctional acid initially added. Mitra et al.[4] developed a procedure for the optimization of industrial semibatch nylon-6 reactor using Sequential Quadratic Programming and Nondominated Sorting Genetic Algorithm. The former method was used to get optimum values for constants, the latter, to obtain improved multiobjective Pareto optimal solutions for three grades of nylon 6. It was used two continuous variables (vapor releasing and jacket temperature) as optimizing variables. Agrawal et al.[5] simulated the nylon-6 hydrolytic polymerization in a VK tube (vertical column) using a plug-flow model and an empirical vapor-liquid equilibrium relation to predict water profile; the predicted values of conversion, molecular weight,

and end group concentrations from the developed model indicated a good agreement with experimental data. Seavey et al.[6] presented a thermodynamically consistent model for the phase equilibrium of water/caprolactam/nylon-6 mixtures based on the poly-NRTL 6 and validated the interaction parameters by performing exploratory simulations of commercial manufacturing processes. The model was applied to simulate a melt train and a bubble-gas kettle train for industrial production of nylon-6. Ramteke and Gupta[7] studied the hydrolytic nylon-6 step-growth polymerization in a semibatch reactor near industrial conditions. It was found that either PolyNRTL or PolyNRF models can be used to describe the vapor–liquid equilibrium. Simulations with tuned parameters have given reasonable agreement for monomer conversion, conversion of water extractibles, and number average chain length.

Experimental design has been successfully applied in polymerization studies to correlate process conditions to conversion and polymer properties. Costa et al.[8] used computational simulation and experimental design to correlate polymer properties to operational parameters in a nylon-6 polymerization in a continuous reactor. Chen[9] used this technique to investigate the influence of chemical oxidation polymerization conditions (time, reactants proportion, and temperature) on the yields of polyaniline powder. Guanaes et al.[10] evaluated the influence of polymerization conditions on the molecular weight and polydispersity of polyepichlorohydrin using a factorial design. Lima et al.[11] studied the free radical solution copolymerization of methyl methacrylate and vinyl acetate in a continuous stirred tank reactor. The factorial planning was used to discriminate the variables with higher impact on the process performance (effects). There were seven process variables and four exits to be evaluated; the screened variables were used to build up a dynamic model based on the functional fuzzy relationship of Takagi–Sugeno type.

As observed, there is a considerable amount of research directed toward analysis, modeling, and simulation of polymerization systems in many kinds of reactors; however, there is still no studies that use experimental design and response surface analysis techniques combined with computational simulation to correlate the influence of operational conditions and reactants charge at the final product properties and process performance (measured by the monomer conversion) in semibatch reactor. The potential advantage of such approach coupling experimental design and response surface analysis with computational simulation is due to the fact that detailed process model may be used to find out optimal and feasible operating regions without considering all the restrictions and process peculiarities.

Bearing this in mind, this work presents the study of the effects of the process variables and feed conditions on the ε-caprolactam conversion (X_{CL}) and nylon-6 number average molecular weight (MWN) in a semibatch reactor through hydrolytic polymerization route. The modeling was based on a nylon-6 polymerization reactor operated on semibatch mode used for polymer research at Biofabris Institute/University of Campinas/Brazil. Responses were obtained by computational simulation using the software Aspen Polymer Plus® 7.4 (Aspen Technology, Burlington, Massachusetts, USA), and experimental design was used to measure factors effects on responses. The analyses were made with the software Statistica 7.0 (Statsoft, Tulsa, OK, USA). Simplified, although statistically representative, models for responses prediction, considering the most important factors (that means process variables), are presented. The main objectives of this work are: (1) to screen the main parameters affecting the monomer conversion (X_{CL}) and MWN in the hydrolytic polymerization of nylon-6 in a semibatch reactor, (2) to generate models for X_{CL} and MWN prediction considering the significant parameters, and (3) to analyze the MWN and X_{CL} behaviors by Response Surface Methodology (RSM).

PROCESS SIMULATION

In the kinetic scheme, the following reactions were considered: ring opening of monomer by water, monomer polyaddition, cyclic dimer (CD) ring opening, CD polyaddition, and acetic acid terminator. The scheme for reactions not involving chain terminators, accepted as standard when regarding ε-caprolactam hydrolytic polymerization, was proposed by Arai et al.[12] The acetic acid chain terminator reaction is the same proposed for Gupta and Kumar.[13]

The modeling approach was expressed in terms of end functional groups and can be found in Table I. All reactions in nylon-6 polymerization takes place under two conditions: uncatalyzed or catalyzed by acid groups (—COOH), both are taking into account in the rate constant expression. Parameters for rate and equilibrium constants, fitted by Arai et al.[12] can be found in Table II. Table III presents the species balance in function of the rates from Table I.

Usually, nylon-6 hydrolytic polymerization is studied taking into account a common industrial configuration based on a continuous process with two reactors. The first one works with high pressure, low temperature, and high water content, preventing devolatilization and promoting oligomers formation. The second one has higher temperature and low pressure to stimulate water removing and, consequently, chain growing by polycondensation reactions. In the semibatch process, this is adapted by introducing profiles of pressure (high in the beginning and vacuum in the last stage) and temperature (ramp heated until temperature reaction). This reactor configuration is interesting to provide more flexibility aiming the development of polymers with specific properties.

The configuration of the reactor considered in this study is shown schematically in Figure 1. The semibatch polymerization reactor consists of a jacketed vessel with an agitator, one stream for vapor releasing and another to collect the final product. The feed consists of the monomer ε-caprolactam (CL), water (*W*), and acetic acid (AA), used as chain terminator. Vapor stream is composed by CL, *W*, and AA. The process has a total operational time of 6 h and works with temperature and pressure profiles, starting at room conditions: temperature of 25°C and pressure of 1 kgf/cm^2. In Aspen Polymer Plus, the RBatch vessel was used to simulate the process.

There is a nitrogen inlet in the experimental process for pressure built in and to avoid thermal-oxidation reactions, but it was not used in the simulation because the Aspen Plus® can

Table I. Reactions and its Rates for Nylon-6 Polymerization

Equilibrium reaction	Reaction rate
Ring opening	
$W + CL \underset{k'_1=\frac{k_1}{K_1}}{\overset{k_1}{\Leftrightarrow}} P_1$	$R_1 = k_1.[CL][W] - k'_1[P_1]$
Polycondensation	
$P_1 + P_1 \underset{k'_2=\frac{k_2}{K_2}}{\overset{k_2}{\Leftrightarrow}} \text{T-COOH} : \text{T-NH}_2 + W$	$R_2 = k_2.[P_1]^2 - k'_2[P_1][W]$
$P_1 + \text{T-COOH} \underset{k'_2=\frac{k_2}{K_2}}{\overset{k_2}{\Leftrightarrow}} \text{T-COOH} : \text{B}-\text{ACA} + W$	$R_3 = k_2[P_1][\text{T-COOH}] - k'_2[W][\text{T-COOH}]\left(\frac{[\text{B}-\text{ACA}]}{[\text{B}-\text{ACA}]+[\text{T}-\text{NH}_2]}\right)$
$P_1 + \text{T-NH}_2 \underset{k'_2=\frac{k_2}{K_2}}{\overset{k_2}{\Leftrightarrow}} \text{T-NH}_2 : \text{B}-\text{ACA} + W$	$R_4 = k_2[P_1][\text{T}-\text{NH}_2] - k_2'[W][\text{B}-\text{ACA}]\left(\frac{[\text{B}-\text{ACA}]}{[\text{B}-\text{ACA}]+[\text{T}-\text{COOH}]}\right)$
$\text{T}-\text{COOH} + \text{T}-\text{NH}_2 \underset{k'_2=\frac{k_2}{K_2}}{\overset{k_2}{\Leftrightarrow}} \text{B}-\text{ACA} : \text{B}-\text{ACA} + W$	$R_5 = k_2[\text{T}-\text{COOH}][\text{T}-\text{NH}_2] - k_2'[W][\text{B}-\text{ACA}]\left(\frac{[\text{B}-\text{ACA}]}{[\text{B}-\text{ACA}]+[\text{T}-\text{NH}_2]}\right)$
Polyaddition of ε-caprolactam	
$CL + P_1 \underset{k'_3=\frac{k_3}{K_3}}{\overset{k_3}{\Leftrightarrow}} \text{T}-\text{NH}_2 : \text{T}-\text{COOH}$	$R_7 = k_3[CL][\text{T}-\text{NH}_2] - k'_3\left(\frac{[\text{B}-\text{ACA}]}{[\text{B}-\text{ACA}]+[\text{T}-\text{COOH}]}\right)$
$CL + \text{T}-\text{NH}_2 \underset{k'_3=\frac{k_3}{K_3}}{\overset{k_3}{\Leftrightarrow}} \text{T}-\text{NH}_2 : \text{B}-\text{ACA}$	$R_6 = k_3[CL][P_1] - k'_3[P_2]$
Polyaddition of cyclic dimer	
$CD + W \underset{k'_4=\frac{k_4}{K_4}}{\overset{k_4}{\Leftrightarrow}} \text{T-NH}_2 : \text{T-COOH}$	$R_8 = k_4[CD][W] - k'_4[P_2]$
$CD + P_1 \underset{k'_{5,m}=\frac{k_5}{K_5}}{\overset{k_5}{\Leftrightarrow}} \text{T-NH}_2 : \text{B}-\text{ACA} : \text{T-COOH}$	$R_9 = k_5[CD][P_1] - k'_5[P_3]$
$CD + \text{T}-\text{NH}_2 \underset{k'_{5,m}=\frac{k_5}{K_5}}{\overset{k_5}{\Leftrightarrow}} \text{T-NH}_2 : \text{B}-\text{ACA} : \text{B}-\text{ACA}$	$R_{10} = k_5[CD][\text{T}-\text{NH}_2] - k'_5[\text{T}-\text{NH}_2].\left(\frac{[\text{B}-\text{ACA}]}{[\text{B}-\text{ACA}]+[\text{T}-\text{COOH}]}\right)$
Polycondensation of acetic acid	
$P_1 + AA \underset{k'_2=\frac{k_2}{K_2}}{\overset{k_2}{\Leftrightarrow}} \text{T}-\text{COOH} : \text{T}-\text{AA} + W$	$R_{11} = k_2.[P_1].[AA] - k'_2.[W][\text{T}-\text{AA}].\left(\frac{[\text{T}-\text{COOH}]}{[\text{B}-\text{ACA}]+[\text{T}-\text{COOH}]}\right)$
$\text{T}-\text{NH}_2 + AA \underset{k'_2=\frac{k_2}{K_2}}{\overset{k_2}{\Leftrightarrow}} \text{B}-\text{ACA} : \text{T}-\text{AA} + W$	$R_{12} = k_2[AA].[\text{T}-\text{NH}_2] - k'_2.[W][\text{T}-\text{AA}]\left(\frac{[\text{B}-\text{ACA}]}{[\text{B}-\text{ACA}]+[\text{T}-\text{COOH}]}\right)$

achieve the specified pressure without this stream and the atmosphere is considered inert.

The configuration of the RBatch vessel allows only two types of inlet streams: one for the charge and one for continuous feed. If the latter were used for the nitrogen feed, it should be defined in the flow profile, which is unknown. As the simulator does not work with the volume of the reactor, it is not possible to specify the initial quantity of N_2 in the process neither the needed flow to reach defined pressures.

The PolyNRTL method was adopted for physical properties calculation in the simulator. It is based on PolyNTRL activity coefficients model and Redlinch–Kwong equation of state for calculation of vapor-phase fugacity coefficients. Details about this methodology and estimated parameters for nylon-6 hydrolytic process can be found at Seavey et al.[6]

FACTORIAL DESIGN APPLIED TO NYLON 6 HYDROLYTIC POLYMERIZATION IN A SEMIBATCH PROCESS

Full factorial designs are important means to evaluate the influence of the factors on responses; however, they have the inconvenience of requiring too many runs when working with a great number of factors. This occurs because the amount of runs increases exponentially with the number of involved variables. The greater the number of variables involved, the higher the

Table II. Rate and Equilibrium Constants (Arai et al.[12])

	Rate constant expression: $k_i = A_i^0 \cdot \exp\left(-\frac{E_i^0}{RT}\right) + A_i^c \cdot \exp\left(-\frac{E_i^c}{RT}\right) \cdot [-COOH] \quad (i = 1, 2, \ldots, 5)$; Equilibrium constant expression: $K_i = \frac{k_i}{k_i^0} = \exp\left(\frac{\Delta S_i - \frac{\Delta H_i}{T}}{R}\right)$					
i	A_i^0 (kg/mol.h)	E_i^0 (J/mol)	A_i^0 (kg^2/mol^2.h)	E_i^c (J/mol)	ΔH_i (J/mol)	ΔH_i (J/mol.K)
1	5.9874×10^5	8.3234×10^4	4.3080×10^7	7.8722×10^4	8.0287×10^3	-3.3005×10^1
2	1.8940×10^{10}	9.7431×10^4	1.2110×10^{10}	8.6525×10^4	-2.4889×10^4	3.9505×10^0
3	2.8560×10^9	9.5647×10^4	1.6380×10^{10}	8.4168×10^4	-1.6927×10^4	-2.9075×10^1
4	8.5778×10^{11}	1.7585×10^5	2.3307×10^{12}	1.5656×10^5	-4.0186×10^4	-6.0781×10^1
5	2.5701×10^8	8.9179×10^4	3.0110×10^9	8.5394×10^4	-1.3266×10^4	2.4390×10^0

chances of some variables did not affect significantly the responses. Therefore, it is interesting to screen the most significant factors before running the full factorial design when there are too many options to be studied; an option is the fractional factorial design.

Fractional factorial designs are experimental designs consisting of a chosen fraction of the experimental runs of a full factorial design that provides almost the same information with only a fraction of runs. There is a lot of information about the highest order interactions (depending of the resolution), but they are hard to be interpreted and, in general, are not significant. The resolution indicates the ability of the design to separate main effects and low-order interactions from each other. To represent the fractional designs, the notation l^{k-p} is used, where l is the number of levels of each investigated factor, k is the number of factors, and p describes the size of the fraction of the full factorial used.[14]

For screening purposes, the influences of process and feed conditions on ε-caprolactam conversion (X_{CL}) and MWN were evaluated by using of four fractional factorial designs of two levels plus one central point. The central point is usually used with repetition for error estimation; however, only one point was used in this case because there are no reproducibility errors in computer simulations. Level zero values were defined based on real procedures developed by Costa[15] and performed in the experimental unit for nylon-6 polymerization previously mentioned in this work.

Table III. Species Balance in Terms of Rates from Table I

Component (*i*)	Species balance for *i*
W	$r_W = R_2 + R_3 + R_4 + R_5 + R_{11} + R_{12} - (R_1 + R_8)$
CL	$r_{CL} = -(R_1 + R_6 + R_7)$
CD	$r_{CD} = -(R_8 + R_9 + R_{10})$
AA	$r_{AA} = -(R_{11} + R_{12})$
P_1	$r_{P_1} = R_1 - (2.R_2 + R_3 + R_4 + R_6 + R_9 + (R_{11})$
B-ACA	$r_{B-ACA} = R_3 + R_4 + 2.R_5 + R_7 + R_9 + 2R_{10} + R_{12}$
T-NH_2	$r_{T-NH2} = R_2 + R_6 + R_8 + R_9 - (R_5 + R_{12})$
T-COOH	$r_{T-COOH} = R_2 + R_6 + R_8 + R_9 + R_{11} - R_5$
T-AA	$r_{T-AA} = R_{11} + R_{12}$

The objective of the first design, 2^{6-2}, was to evaluate all the feed and process variables, individually. The charging variables were the initial charge of ε-caprolactam (m_{CL}), water (m_W), and acetic acid (m_{AA}). The process variables used were: pressure in the high pressure stage (HP), pressure in the vacuum stage (LP), and reaction temperature (T), defined as the maximum value in the temperature profile. Values for each level are presented in Table IV.

A process temperature profile with four stages was established. The process starts at room temperature (25°C), reaches the temperatures $T_{1\ h}$ in 1 h, $T_{2\ h}$ at 2 h and $T_{3\ h}$ in 3 h, value that is kept constant until the end of the reaction. Once T is set, $T_{2\ h}$ is calculated as 110°C below T, and $T_{1\ h}$ as 90°C below $T_{2\ h}$. Table V contains the simulated temperature profiles in each reaction temperature (T) level (valid for all fractional designs).

The pressure profile has five stages. Initially, the pressure is maintained at 1 kgf/cm^2 for 1 h. Then, it is increased and reaches HP value after 2 h of reaction. After 1.5 h of constant pressure, the pressure ramps down for 0.5 h until reaches LP

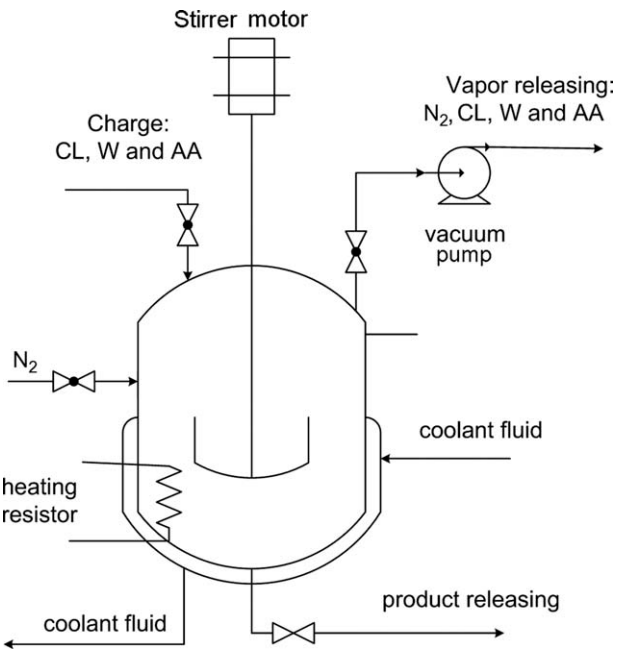

Figure 1. Experimental semibatch reactor used for nylon-6 hydrolytic polymerization.

Table IV. Factors Used in the 2^{6-2} Fractional Design

	Level		
Factor	−1	0	1
High pressure (HP, kgf/cm^2)	3	5	7
Low pressure (LP, kgf/cm^2)	0.25	0.50	0.75
Reaction temperature (T, °C)	240	260	280
Mass of ε-caprolactam(m_{CL}, g)	800	1000	1200
Mass of water (m_W, g)	25.70	32.12	38.54
Mass of acetic acid (m_{AA}, g)	0	3.1	6.2

and is held in this value until the end of the process. Table VI presents how the pressure profile was defined in the simulator.

As the responses are dependent on a set of chemical reactions, it is interesting to know if the proportion of reactants in the charge can significantly affect them. To study this, a set of three 2^{5-1} designs was proposed. They have all the same operational variables of the 2^{6-2} experimental design (HP, LP, and T), but instead of the quantity of reactants, the charge variables were the molar ratio between reactants. Each one of the designs has the mass of one of the reactants maintained constant and varies the other two. The experimental designs were denominated as A (ε-caprolactam constant), B (water constant), and C (acetic acid constant). Their factors and values for each level are available in Table VII.

The results for the 2^{6-1} and three 2^{5-1} fractional factorial designs, obtained by simulation, were analyzed by using of the software STATISTICA (Statsoft v. 7.0).

Screening of Factors Affecting Nylon-6 MWN

For screening purposes, the responses obtained for conversion of ε-caprolactam were evaluated by using of the Pareto chart (Figures 2–5). At the Pareto chart, all factor effects are represented by horizontal bars. In fact, the bars do not show the value of the effects, but $t(v)$, which is the ratio of the estimated effects to the standard deviation and v is the number of degrees of freedom. The physical interpretation of effect values is that they are the measure of the change in the response when the factors are moved from an inferior to superior level. There is also a vertical line that represents the effect's limit of significance; bars before that line are considered not statistically significant. The line position depends on the chosen confidence limit, in this study, 95% ($P = 0.05$) for all cases.

Table V. Data Inserted in the Simulator to Define Temperature Profile for Each T Level Used in All Fractional Factorial Designs

	Level		
Time (h)	−1	0	1
0	25	25	25
1	40	60	80
2	130	150	170
3	240	260	280

Table VI. Pressure Profile Inserted in Simulator

Time (h)	Pressure (kgf/cm^2)
0	1
1	1
2	HP
3.5	HP
5	LP

As can be seen in all the Pareto charts, the reaction temperature (T) was considered statistically significant in all the experimental designs performed. The 2^{6-2} planning indicated that acetic acid was also relevant to MWN response, information confirmed in the $2^{5-1}A$ and B designs, in which the relations AA/CL and AA/W appeared as significant. In $2^{5-1}C$ design, where the quantity of acetic acid was not changed, none of the reactants ratio to AA appeared to be significant but a different factor, HP, was revealed to be important to MWN build up.

It was expected that the low pressure value could have some influence on this response, as it affects water evaporation and, consequently, the polycondensation reaction equilibrium. As can be seen in the results, it did not happen, maybe because either the chosen range was too restrict or the operational time in low pressures was too short to have significant effect on MWN response.

Considering preliminary experimental designs results for MWN, a complete 2^3 factorial design was proposed having T, HP, and AA/CL as variables, to obtain a statistical model. Decodified values for the variables can be found in Table VIII. As the AA/CL and AA/W ratios were both important and had similar effects in magnitude and signal, water and ε-caprolactam mass were established at 31.84 and 1000 g, respectively, and only AA/CL ratio was changed. The low pressure value was also set at 0.5 kgf/cm^2 (level zero value of the previous plannings). Table IX outlines the experimental design and results obtained for MWN.

Figure 6 depicts the Pareto chart for MWN considering a confidence level of 95%. In this time, the analysis was performed

Table VII. Factors and their Levels Used in the 2^{5-1} Experimental Designs

		Level		
Experimental design	Factor	−1	0	1
All	HP	3	5	7
	LP	0.25	0.5	0.75
	T	240	260	280
A ($m_{CL} = 1000$ g)	W/CL[a]	0.1	0.2	0.3
	AA/CL[a]	0.002	0.006	0.01
B ($m_W = 31.84$ g)	CL/W[a]	4	5	6
	AA/W[a]	0.01	0.03	0.05
C ($m_{AA} = 3.18$ g)	CL/AA[a]	113.3	167	200
	W/AA[a]	16.6	33.3	50

[a]Molar ratio.

Applied Polymer SCIENCE

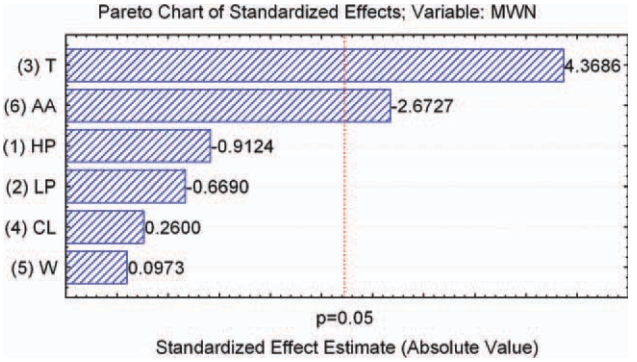

Figure 2. Pareto chart of effects for MWN in design 2^{6-2} [Color figure can be viewed in the online issue, which is available at wileyonlinelibrary.com.]

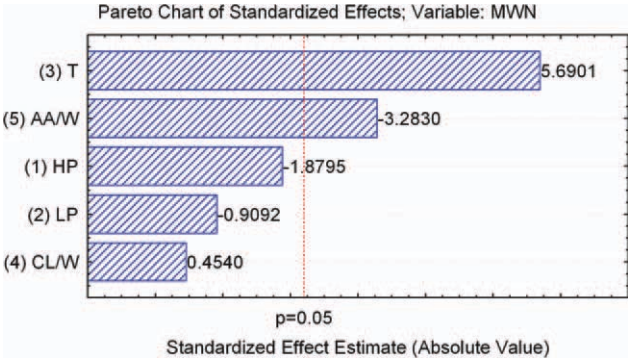

Figure 4. Pareto chart of effects for MWN in design 2^{5-1} *B* [Color figure can be viewed in the online issue, which is available at wileyonlinelibrary.com.]

considering a two-way interaction model. According to the estimated effects, the reaction temperature (*T*) and the acetic acid concentration (AA) were the most important ones (largest absolute magnitudes). After the screening process, almost all factors have shown to be statistically significant, the only exception was the interaction between AA and HP.

As expected, the temperature has positive effect on MWN because interferes in the polymerization kinetics, increasing reaction rates and, consequently, the molecular weight. The acetic acid works in the opposite way, limiting the molecular weight. This can be explained because the nylon-6 chains have two reaction sites, NH_2 and COOH terminal groups, and, when the former reacts with acetic acid, not only one of the sites is deactivated but also the molecule chain cannot grow up by polyaddition mechanism.

Presumably, the effect of *T* and AA/CL interaction is important due to the rising of acetic acid conversion by temperature increasing. The negative effect of HP on MWN is probably because the higher the pressure, less acetic acid is lost by vaporization and more of this reactant, which has negative effect on MWN, is present in the reaction medium.

Simplified Model for MWN

A new statistical analysis was made neglecting the insignificant effect and a model with the significant effects was generated.

Table X outlines the calculated effects on MWN and the coefficients of the model, exposed on eq. (1) and where the variables *T*, HP, and molar ratio AA/CL are in the coded form.

$$\begin{aligned}\mathrm{MWN} = {} & 14043.6 + 5362.5 \times T - 1688.6 \\ & \times \mathrm{HP} - 2958.3 \times (\mathrm{AA/CL}) - 1492.7 \\ & \times \mathrm{HP} \times T - 2519.3 \times T \times (\mathrm{AA/CL}) \quad (1)\end{aligned}$$

To ensure that the generated model has statistical significance, the analysis of variance (ANOVA) was performed for MWN, which can be found in Table XI. The response has a correlation coefficient (R^2) equal to 0.9937, value very close to unit and that indicates good adjustment to data. The *F*-test shows that the model is reliable, as the calculated *F*-value is 10.57 times larger than the listed value for a 95% confidence level (as a practical rule, the model has statistical significance when the calculated *F*-value is at least five times larger than the listed value). The accuracy of the model can be visualized by a comparison between the responses predicted by the deterministic model (simulation) and those calculated by the reduced model, depicted in Figure 7.

As the model has a good agreement with simulation data, it can be used in the future for optimization purposes, when validated with experimental data. In polymerizations processes, more

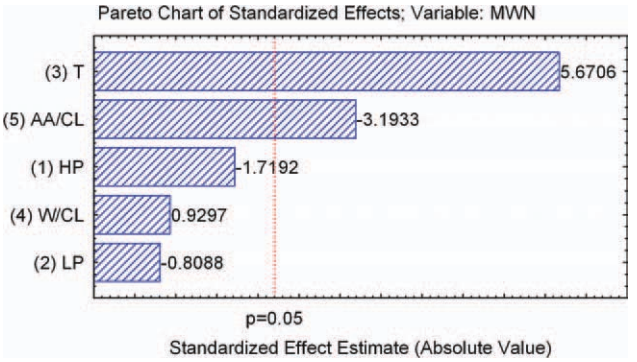

Figure 3. Pareto chart of effects for MWN in design 2^{5-1} *A* [Color figure can be viewed in the online issue, which is available at wileyonlinelibrary.com.]

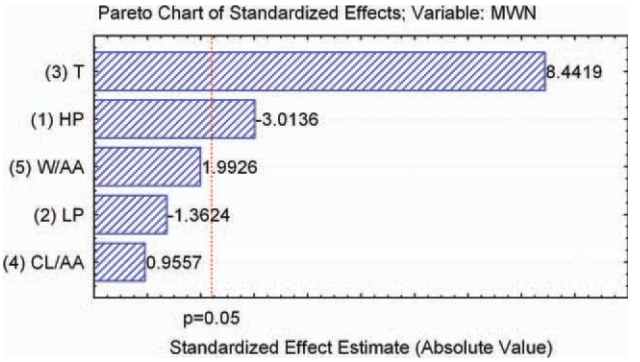

Figure 5. Pareto chart of effects for MWN in design 2^{5-1} *C* [Color figure can be viewed in the online issue, which is available at wileyonlinelibrary.com.]

Table VIII. Factors Used in the 2^3 Fractional Design

	Level		
Factor	−1	0	1
High pressure (HP, kgf/cm^2)	3	5	7
Reaction temperature (T, °C)	240	260	280
AA/CL (molar ratio)	0.002	0.006	0.010

important than to attain a product with elevated molecular weight is having a material with adequate properties. For example, long polymer chains are related to an increasing of viscosity and this can became a real problem in some cases. The eq. (1) can be used to find the best set of variables that will give the desired value of MWN and that attends some specified conditions like higher conversion (working with the X_{CL} model), lower temperature, etc.

Surface Response Analysis for MWN

Due to the reliability of the statistical model [eq. (1)], it was used to generate the response surfaces plotted in Figures 8–10. These kinds of graphs map the behavior of the dependent variable when varying the independent variables in the available range. Thus, they are useful for identification of the optimal region, as they indicate to which direction the dependent variable gets near to the optimum. The color/tones in the graph illustrate the magnitude of the response: higher values are found in the dark tones region, while the lower values are represented by lighter colors. Above the surface, there is its projection, which provides another way to visualize response values.

As there are three factors and each graph can represent only two independent variables at a time, two variables were selected to vary at a time and the other one was maintained at central point.

In this case, it can be seen that a maximum global could not be found for the studied range. This was expected, as this is not a quadratic model. The reaction temperature, T, has a major role in MWN formation, when compared with the other two factors (HP and AA/CL). This can be easily noted when they are held constant and only temperature varies: there is an accentuated inclination when moving from a level to another. In addition, when the reaction temperature is set in the lowest value, a monotonic feature can be observed and the MWN cannot reach values higher than 10,000 no matter in which level is the other variable (confirming the importance of reaction temperature interaction with the other factors). In general, the global analysis of the three surface responses indicates that increasing of MWN is promoted by higher values of T and lower values of HP and AA/CL.

Table IX. 2^3 Design Matrix Used for Determining of MWN Model

	Factor			Response	
Run	T	HP	AA/CL	X_{CL}	MWN
1	−1	−1	−1	64.90	9004
2	1	−1	−1	79.21	28,027
3	−1	1	−1	86.45	9525
4	1	1	−1	87.09	22,029
5	−1	−1	1	81.84	9039
6	1	−1	1	83.40	17,436
7	−1	1	1	89.30	7734
8	1	1	1	87.59	10,709
9 (C)	0	0	0	88.36	12,890

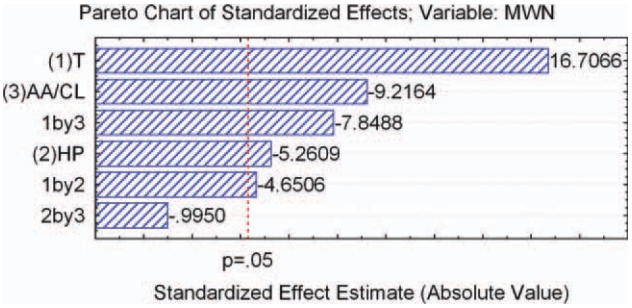

Figure 6. Pareto chart of effects for MWN (at 95% confidence level) [Color figure can be viewed in the online issue, which is available at wileyonlinelibrary.com.]

When choosing the work range for T, it has to be taken into account that simulations at central point revealed that ε-caprolactam consumption starts only after reactor temperature reaches ∼ 200°C; therefore, the lowest level had to be above that value. Also, high temperatures are not desirable when working with polymers. Thermogravimetry analysis in literature[16] indicated that nylon-6 degradation is accentuated after 350°C; thus, the superior limit needed to be a value below it and considering a margin of safety.

Screening of Factors Affecting ε-Caprolactam Conversion (X_{CL})

Figures 11–14 show the Pareto charts for 2^{6-2}, $2^{5-1}A$, B, and C fractional factorial designs for X_{CL} response.

According to the Pareto charts, HP is statistically significant in all of the experimental designs performed. Besides HP, it appeared as relevant factors the ratio between acetic acid to ε-caprolactam (2^{5-1} A) and the mass of acetic acid in 2^{6-2} design. Even the reaction temperature did not appear as statistically significant at 95% confidence, we decided not to discard it, because the designs indicate that T has the third or second most important standard effect on X_{CL} and also, in the first

Table X. Effect Estimates on MWN from Results of the 2^3 Design: Variables with Significant Effects[a]

Factor	Effect	$t(3)$	P	Coefficient
Mean/intercept	14,044	46.48	0.0000	14,043.6
T	10,725	16.73	0.0005	5362.5
HP	−3377	−5.27	0.0133	−1688.6
AA/CL	−5917	−9.23	0.0027	−2958.3
T × HP	−2985	−4.66	0.0187	−1492.7
T × AA/CL	−5039	−7.86	0.0043	−2519.3

[a]Significant factors ($P < 0.05$) for a 95% confidence level.

Table XI. Analysis of Variance for the MWN Regression: Reduced Model (ANOVA)

Source of variation	Sum of squares	Degrees of freedom	Mean square	*F*-value	*F*-test/$F_{0.95;5.3}$
Regression	391,473,774	5	78,294,755	95.307	10.57
Residual	2,464,515	3	821,505		
Total	393,938,289	8			

$R^2 = 0.9937$, $F_{0.95;5,3} = 9.0135$ (listed).

design, its absolute standard effect is very near to the cut-off line for significant effects.

Considering preliminary experimental designs results for X_{CL}, a complete 2^3 factorial design was proposed having *T*, HP, and AA as variables to obtain a statistical reduced model. All the insignificant variables were set at the same value of level zero in previous experiments. As these were the same factors analyzed to obtain the MWN model, it was used the same experimental design, but only HP appeared as significant for X_{CL}, and it was not possible to attain a significant model working only with it.

Supposing that the lack of adjustment of the model was due to a quadratic behavior, a new central composite design was performed including the eight factorial points and the central point (both of the previous planning) plus a star configuration (six axial points), totalizing 15 runs. The star configuration requires $2n$ additional runs besides those of the factorial design, where n is the number of independent variables. The purpose of introducing these additional runs is to generate a quadratic model for responses; they are related to the process response when all factors are in the central point except one, which is at $\pm\alpha$ level. The α value is calculated based on the number of factors and corresponds to $(2^n)^{1/4}$. In this case, there are three factors; therefore, $\alpha = 1.682$.

After analyzing the obtained data, it was observed that a statistical significant model was not achieved. With the purpose of obtaining a good reduced model for ε-caprolactam conversion, some changes in the design were performed: HP and reaction temperature (*T*) ranges were reduced, and the central point was dislocated. The values of the factors and obtained results for the final composite design are shown in Tables XII and XIII, respectively.

Figure 15 depicts the Pareto chart for X_{CL} considering a confidence level of 95%. The analysis was performed considering linear (*L*) and quadratic (*Q*) main effects plus two-way interactions model. According to the estimated effects, linear HP, *T*, and AA/CL effects are the most important to X_{CL} response, respectively. HP and *T* quadratic terms and interaction between *T* and AA/CL were also considered relevant.

Simplified Model for X_{CL}

Considering composite design results, a new statistical analysis was made neglecting the insignificant effects and a model considering only significant effects was generated. Table XIV outlines the calculated effects on X_{CL} and the coefficients of the model, exposed on eq. (2). It is important to emphasize that the equation variables are in the coded form.

$$X_{CL} = 8.9889 + 0.6943 \times HP - 0.1219 \times HP^2 - 0.4052 \times T - 0.3186 \times T^2 + 0.3095 \times AA - 0.1636T \times AA \quad (2)$$

When dealing with conversion, the optimal value is always the highest and the eq. (2) can be used to help the identification of the best set of *T*, AA/CL, and HP values that leads to desired X_{CL} underspecified conditions.

Table XV presents the ANOVA for X_{CL}. The response has as correlation coefficient (R^2) equal to 0.9812, which means that 99%

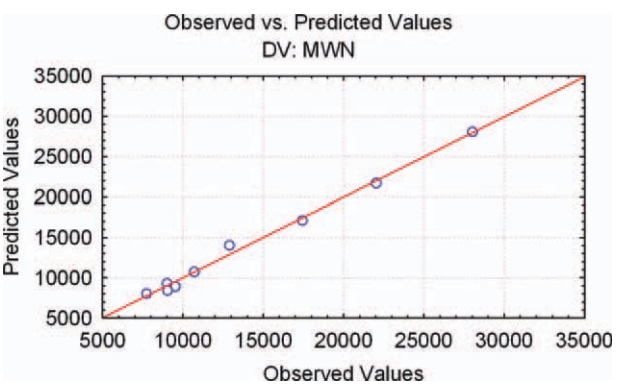

Figure 7. Comparison between MWN responses obtained by computational simulation (observed values) versus predicted values by the reduced statistical model [Color figure can be viewed in the online issue, which is available at wileyonlinelibrary.com.]

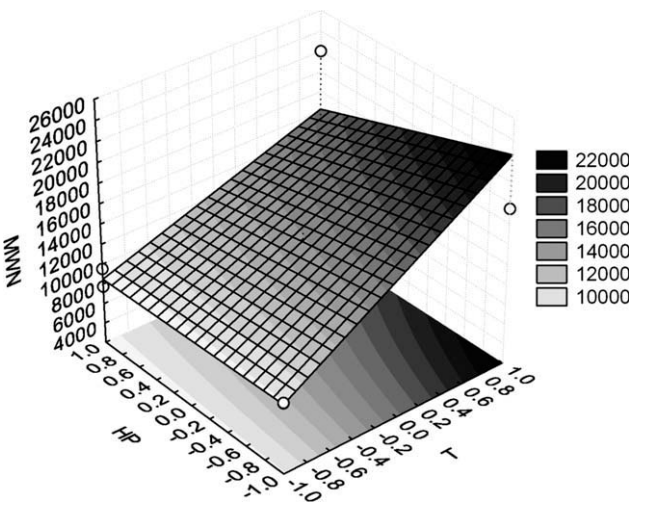

Figure 8. Response surface for MWN as a function of HP and *T*.

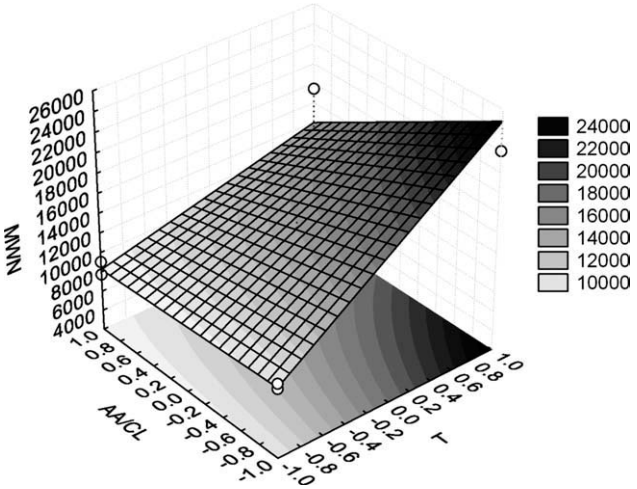

Figure 9. Response surface for MWN as a function of AA/CL and *T*.

of the variance is explained by the model. The *F*-test confirmed that the model is reliable, as the calculated *F*-value is 14.55 times larger than the listed value for a 95% confidence level. The accuracy of the model can be visualized by a comparison between the responses predicted by the deterministic model (simulation) and those calculated by the reduced model, depicted in Figure 16.

Response Surface Analysis for X_{CL}

The fitted response surfaces considering the model for conversion are shown in Figures 17–19. When dealing with conversion, the optimal values are always those with the highest values. As a quadratic model was used, there was a probability to find an optimal point for X_{CL} in the studied ranges. Although the graphs did not show an optimal global, it was possible to visualize optimal tendencies.

It can be seen that higher HP values always lead to higher conversions, which can be explained by its effect on evaporation

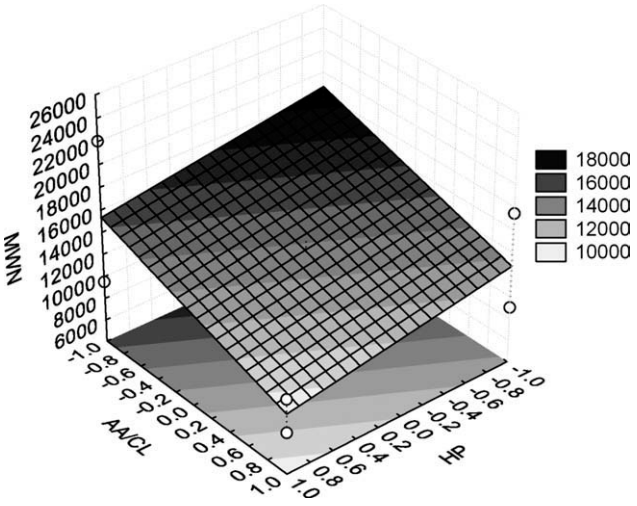

Figure 10. Response surface for MWN as a function of AA/CL and HP.

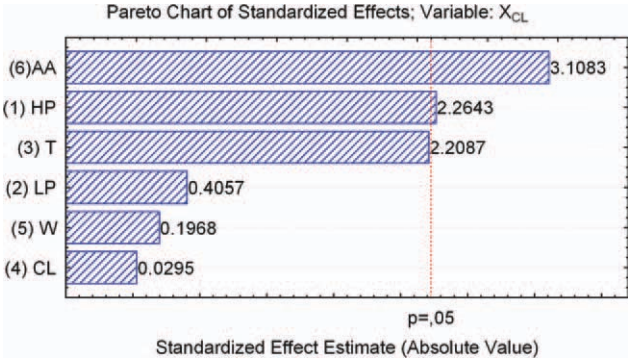

Figure 11. Pareto chart of effects for X_{CL} in design 2^{6-2} [Color figure can be viewed in the online issue, which is available at wileyonlinelibrary.com.]

rates, preventing loss of monomer. The reaction temperature (*T*) has an accentuated quadratic behavior, and it is possible to identify its optimal value about 270°C (+1 in codified value) in Figures 17 and 19. Low temperatures are not favorable to ε-caprolactam reaction, on the other hand, high temperatures accelerate kinetics reaction but results in a rising of evaporation rates, reducing the availability of monomer in the reactor. The optimal *T* values are those that better conciliate these two effects to obtain a maximum X_{CL}.

The AA/CL has positive effect on X_{CL} when moving from an inferior to a superior level, although changes on response are almost indistinguishable at the superior *T* level. The effect on conversion is probably due to the acid catalyzed kinetics reaction, while the interaction with temperature can be explained by its influence on acetic acid evaporation.

One of the uses of the model can be the multiobjective optimization problem when it is desirable to find the best set of conditions that allows the process to achieve a specified MWN, whereas keeping higher conversion values. It is important not to ignore that each model was designed to work in a specific range for each independent variable, so the optimization have to consider only the range valid for both models.

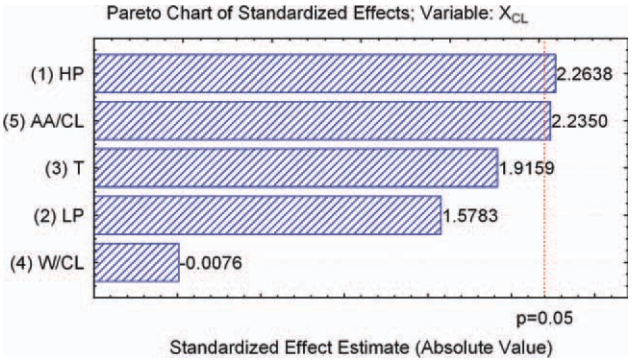

Figure 12. Pareto chart of effects for X_{CL} in design 2^{5-1} *A* [Color figure can be viewed in the online issue, which is available at wileyonlinelibrary.com.]

Applied Polymer SCIENCE

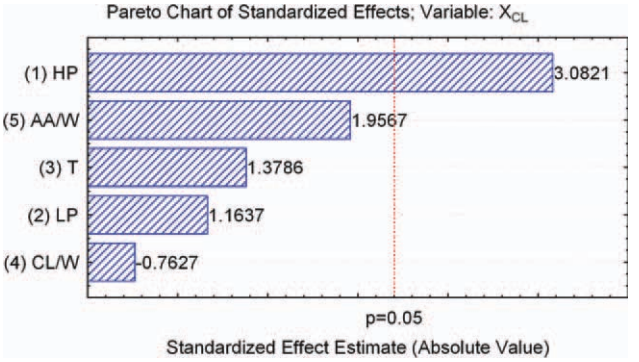

Figure 13. Pareto chart of effects for X_{CL} in design 2^{5-1} *B* [Color figure can be viewed in the online issue, which is available at wileyonlinelibrary.com.]

CONCLUSIONS

This work pointed out that experimental designs and RSM combined with modeling and simulation can be applied for optimization of complex processes like the hydrolytic polymerization of nylon-6 in a semibatch reactor, in which there are many parallels reactions occurring at the same time and profiles of pressure and temperature were applied.

Factorial designs were applied for the screening of the most relevant factors in the studied process considering the final monomer conversion (X_{CL}) and MWN as responses. It was found that the temperature reaction (*T*), the pressure in the high pressure stage (HP), and the ratio of acetic acid to ε-caprolactam (AA/CL) have the most significant effects for both responses. The experimental design allowed the development of reduced models [eqs. (1) and (2)] for responses prediction and their reliability was proved by ANOVA. At the end, response surfaces were obtained by nonlinear multiple regression of the data. They have showed an important tool for optimization purposes by allowing an easier identification of the optimum values, when compared with a rigorous model. It is noteworthy that, even if the same set of significant variables was obtained for the two evaluated responses, the variables work in opposite way on each response in the studied ranges. Although higher pressure values leads to higher monomer conversion, the MWN is

Table XII. Factors Used in the 2^3 Fractional Design

	Level				
Factor	−1.682	−1	0	1	1.682
High pressure (HP, kgf/cm^2)	4.32	3	5	7	7.68
Reaction temperature (*T*, °C)	243	250	260	270	277
AA/CL (molar ratio)	0.0009	0.003	0.006	0.009	0.0111

Table XIII. Central Composite Design Used for Determining of X_{CL} model

	Factor			Response
Run	*T*	HP	AA/CL	X_{CL}
1	−1	−1	−1	87.71
2	−1	−1	1	88.74
3	−1	1	−1	87.44
4	−1	1	1	87.78
5	1	−1	−1	89.31
6	1	−1	1	90.12
7	1	1	−1	88.62
8	1	1	1	88.81
9	−1.682	0	0	87.34
10	1.682	0	0	89.89
11	0	−1.682	0	88.74
12	0	1.682	0	87.38
13	0	0	−1.682	88.31
14	0	0	1.682	89.41
15 (C)	0	0	0.000	89.20

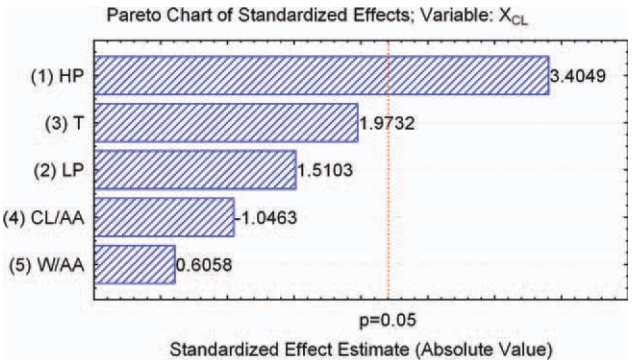

Figure 14. Pareto chart of effects for X_{CL} in design 2^{5-1} *C* [Color figure can be viewed in the online issue, which is available at wileyonlinelibrary.com.]

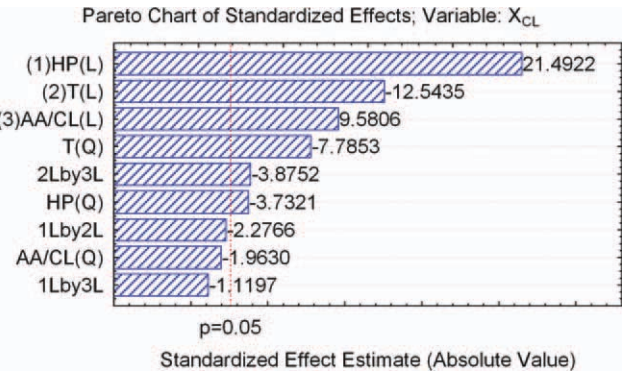

Figure 15. Pareto chart of effects for X_{CL} in central composite design [Color figure can be viewed in the online issue, which is available at wileyonlinelibrary.com.]

Table XIV. Effect Estimates on X_{CL} from Results of the Composite Design: Variables with Significant Effects

Factor	Effect	Standard error	*t*(8)	*P*	Coefficient
Mean/intercept	88.9889	0.0903	985.833	0.0000	88.9889
HP(*L*)	1.3886	0.0893	15.546	0.0000	0.6943
HP(*Q*)	−0.2438	0.1051	−2.320	0.0490	−0.1219
T(*L*)	−0.8105	0.0893	−9.073	0.0000	−0.4052
T(*Q*)	−0.6371	0.1051	−6.063	0.0003	−0.3186
AA(*L*)	0.6190	0.0893	6.930	0.0001	0.3095
T(*L*) × AA(*L*)	−0.3271	0.1167	−2.803	0.0231	−0.1636

Table XV. Analysis of Variance for the X_{CL} Regression: Reduced Model (ANOVA)

Source of variation	Sum of squares	Degrees of freedom	Mean square	*F*-value	*F*-value/ $F_{0.95;6.8}$
Regression	11.3499	6	1.8917	69.442	14.550
Residual	0.2179	8	0.0272		
Total	11.5678	14			

$R^2 = 0.9812$, $F_{0.95;6,8} = 4.7725$ (listed)

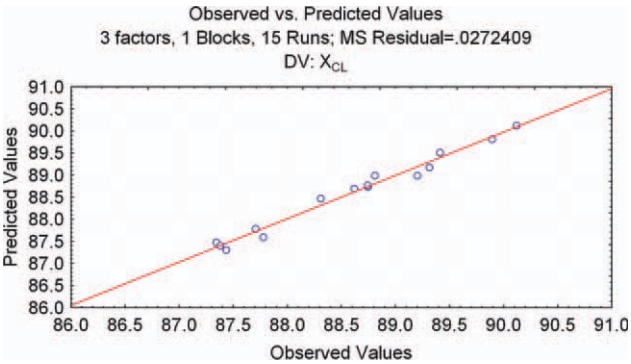

Figure 16. Comparison between X_{CL} responses obtained by computational simulation (observed values) versus predicted values by the reduced statistical model [Color figure can be viewed in the online issue, which is available at wileyonlinelibrary.com.]

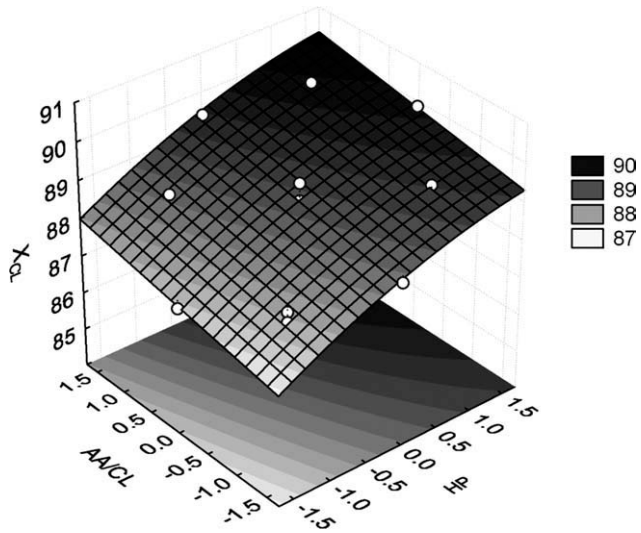

Figure 18. Response surface for X_{CL} (%) as a function of AA/CL and HP.

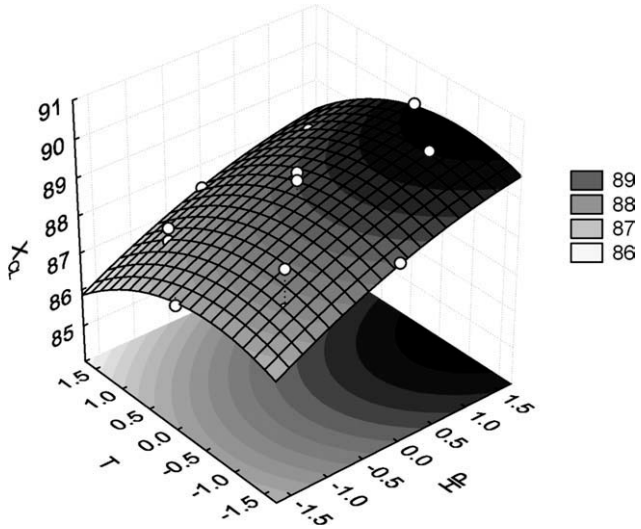

Figure 17. Response surface for X_{CL} (%) as a function of *T* and HP.

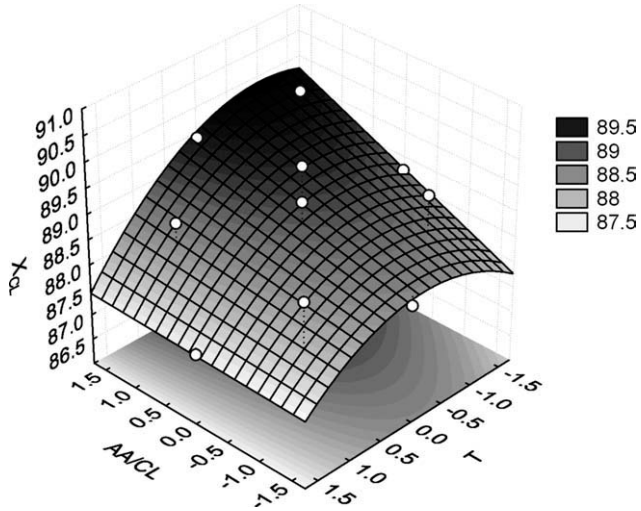

Figure 19. Response surface for X_{CL} (%) as a function of AA/CL and *T*.

reduced in these cases and the same behavior is observed with AA/CL. Changing the reaction temperature from an inferior to a superior level has positive and strong effect on molecular weight, but its effect on conversion may vary and an optimal value can be found in the region around level +1 (270°C).

In this study, only MWN and X_{CL} were evaluated, but other responses might have been considered in the optimization as, for example, the concentration of undesirable CD and reaction time.

Additionally, some limitation was observed regarding the analysis of the ε-caprolactam conversion behavior, so that it may bring difficulties to use such variable to control and optimize the process. Bearing this in mind, this work looked for to understand more closely the behavior of ε-caprolactam conversion as well to investigate the possible use of the temperature profile of the reactor as a potential variable to control and optimize the process.

NOMENCLATURE

AA	Acetic acid
AA/CL	Molar ratio of acetic acid to ε-caprolactam
CD	Cyclic dimer
CL	ε-caprolactam
HP	Pressure of the high pressure stage (kgf/cm^2)
LP	Pressure of the vacuum stage (kgf/cm^2)
m_i	Mass of component *i* (g)
MWN	Number average molecular weight
n	Number of independent variables
T-NH_2	Amine termination
T-COOH	Acid termination
T-AA	Acetic acid termination
X_{CL}	Conversion of e-caprolactam (%)
W	Water

REFERENCES

1. Kohan, M. I. In: Ullmann's Encyclopedia of Industrial Chemistry, Vol. *A-21*; Ullmann, F., Eds.; Deerfield Beach: VCH, **1985;** pp 179–203.
2. Wajge, R. M.; Rao, S. S.; Gupta, S. K. *Polymer* **1994,** *35*, 3722.
3. Tang, Z.-L.; Lin, J.; Huang, N.-X.; Fantoni, R. F. *Angew. Makromol. Chem.* **1997,** *250*, 1.
4. Mitra, K.; Deb, K.; Gupta, S. K. *J. Appl. Polym. Sci.* **1998,** *69*, 69.
5. Agrawal, A. K.; Devika, K.; Manabe, T. *Ind. Eng. Chem. Res.* **2001,** *40*, 2563.
6. Seavey, K. C.; Khare, N. P.; Liu, Y. A.; Williams, T. N.; Chen, C. C. *Ind. Eng. Chem. Res.* **2003,** *42*, 3900.
7. Ramteke, M.; Gupta, S. K. *Ind. Eng. Chem. Res.* **2008,** *47*, 9061.
8. Costa, M. C. B.; Barbosa, M. I. R.; Jardini, A. L.; Embiruçu, M.; Filho, R. M. *Comput.-Aided Chem. Eng.* **2009,** *27*, 1107.
9. Chen, C.-H. *J. Appl. Polym. Sci.* **2002,** *85*, 1571.
10. Guanaes, D.; Bittencourt, E.; Eberlin, M. N.; Sabino, A. A. *Eur. Polym. J.* **2007,** *43*, 2141.
11. Lima, N. M. N.; Filho, R. M.; Embiruçu, M.; Maciel, M. R. W. *J. Appl. Polym. Sci.* **2007,** *106*, 981.
12. Arai, Y.; Tai, K.; Teranishi, H.; Tagawa, T. *Polymer* **1981,** *22*, 273.
13. Gupta, S. K.; Kumar, A. Reaction Engineering of Step-Growth Polymerization; Plenum Press: New York, **1987.**
14. Montgomery, D. C. Design and Analysis of Experiments; Wiley: New York, **2001.**
15. Costa, M. C. B. D.Sc. Thesis, FEQ/Universidade Estadual de Campinas, Campinas, Brazil, **2009.**
16. Shamsuri, A. A.; Daik, R.; Ahmad, I.; Jumali M. H. *J. Polym. Res.* **2009,** *16*, 381.